Ab initio investigation of FeAs/GaAs heterostructures for potential spintronic and superconducting applications

Sinéad M. Griffin*
Materials Department, University of California, Santa Barbara, Santa Barbara, California 93106-5050, USA and Materials Theory, ETH Zurich, CH-8093 Zurich, Switzerland

Nicola A. Spaldin†
Materials Theory, ETH Zurich, CH-8093 Zurich, Switzerland

(Received 29 August 2011; published 16 April 2012)

Ultrathin FeAs is of interest both as the active component in the recently identified pnictide superconductors and in spintronic applications at the interface between ferromagnetic Fe and semiconducting GaAs. Here we use first-principles density-functional theory to investigate the properties of FeAs/GaAs heterostructures. We find that the Fermi surface is modified from that characteristic of the pnictide superconductors by interactions between the FeAs layer and the As atoms in the GaAs layers. Regardless of the number of FeAs layers, the Fe to As ratio, or the strain state, the lowest-energy magnetic ordering is always antiferromagnetic, offering an explanation for the failure of spin injection across Fe/GaAs interfaces. However, such antiferromagnetic layers could be incorporated into heterostructures as an exchange-bias layer.

DOI: 10.1103/PhysRevB.85.155126 PACS number(s): 73.40.−c, 74.78.Fk, 85.75.−d, 74.70.Xa

I. INTRODUCTION

Much attention has been focused on FeAs-based materials, first due to their potential as magnetic semiconducting systems[1–5] and more recently for their unexpected high-T_c superconductivity.[6] Magnetic semiconducting systems are of interest because they could in principle enable so-called spintronic devices that exploit the spin degree of freedom of the electron as well as its charge.[7] One route to spintronic behavior is through hybrid structures in which magnetic metals are used to inject spin-polarized electrons into semiconductors.[8] Here the Fe/GaAs system is particularly appealing because of the high ferromagnetic Curie temperature of Fe, the well-established semiconducting properties of GaAs, and the close lattice match between body-centered-cubic Fe and zinc-blende GaAs. However, spin injection in Fe/GaAs has not yet been proven successful.[9] One possible reason for this is the formation of other phases at the interface; indeed FeAs and Fe_2As have both been reported experimentally[10–13] and *ab initio* calculations suggest that Fe penetrates the GaAs lattice, breaking the Ga-As bonds in favor of Fe-As bonds and elemental Ga.[14]

The recent and entirely unanticipated discovery of superconductivity at ∼50 K in layered rare-earth oxide/iron arsenide compounds has generated tremendous excitement within the condensed-matter community.[15,16] Previously, all known conventional high-temperature (high-T_c) superconductors contained copper-oxygen layers; in fact, the presence of oxygen and the absence of magnetism were believed to be requirements for high-T_c behavior.[17,18] In the current materials, however, superconductivity occurs in the magnetic iron-arsenic planes, in complete violation of the previous understanding; they therefore provide an invaluable tool for exploring the long-sought-after mechanism underlying high-temperature superconductivity. Density-functional calculations have revealed correlations between the superconducting Curie temperature and the normal-state structural and electronic properties of the fluorite-structure Fe-As layer. In particular, the out-of-plane Fe-As bond length, the striped antiferromagnetic order of the undoped parent compound, and the Fermi surface nesting that occurs between bands derived from Fe *d* states seem to be important.

In this work we use first-principles density-functional theory to calculate the structural stabilities and electronic properties of a range of FeAs/GaAs superlattices. The goal of our work is twofold: first, to search for superlattices within this family with desirable spintronic properties such as half metallicity or ferromagnetism and second, to explore whether the signature electronic properties of the FeAs layers in the pnictide superconductors can be reproduced in this artificial system. Our model heterostructures consist of n layers ($n = 1,2,3$) of zinc-blende GaAs alternating with m layers ($m = 1,2,3$) of FeAs in either the zinc-blende structure or the antifluorite structure found in the FeAs superconductors. Here n:m gives the ratio of Fe:Ga in the heterostructure.

II. COMPUTATIONAL DETAILS

Our density-functional theory (DFT) calculations were performed using the Vienna *ab initio* Simulation Package (VASP).[19,20] We expanded the electronic wave functions and density using a plane-wave basis set and used the supplied VASP PAW potentials[21] with the PBE exchange-correlation functional[22,23] for core-valence separation. A $10 \times 10 \times 10$ Monkhorst-Pack[24] k-point mesh with a Gaussian smearing of 0.2 eV was used for the Brillouin zone integrations; these are suitable values for metals. The plane-wave cutoff was set to 400 eV, and for structural relaxations we allowed the ions to relax until the Hellmann-Feynman forces were less than 1 meV/Å^{-1}.

We treated the exchange-correlation functional within the spin-polarized generalized gradient approximation plus Hubbard U (GGA + U) method[25] to account for electron correlations and chose a U of 0.5 eV as implemented in the

Dudarev scheme. While there has been much discussion in the literature of the relative appropriateness of various functionals (hybrids, LDA plus Hubbard U method, GGA + U, etc.) and U parameters, we find that GGA + U with $U = 0.5$ eV gives good agreement with both hybrid functional calculations and experimental structural properties for bulk MnP-type FeAs.[26] In common with all functionals that have been tested to date, the local magnetic moments are overestimated compared with those reported experimentally;[27] it remains a matter of debate whether this is a consequence of the neglect of spin fluctuations in the density-functional formalism[28] and/or the difficulties associated with rigorously defining a local moment experimentally in such a broadband metallic system[29] The magnetic moments are calculated by projecting the plane-wave states into the PAW sphere of the magnetic ions (in this case, Fe).

III. RESULTS: BULK PROPERTIES OF FeAs and Fe_2As

A. Properties of bulk FeAs in MnP and ZnS structural variants

We begin with a comparison of bulk FeAs in its experimentally observed ground-state MnP structure[30] and the zinc-blende structure that is of interest for our spintronic superlattice calculations. Figure 1 shows the structures of the MnP-type and zinc-blende FeAs. The former [Fig. 1(a)] consists of octahedrally coordinated Fe ions with the octahedra edge shared. The octahedra are distorted with the Fe ions shifted from their centers. In both cases the magnetic ground state is antiferromagnetic (AFM), indicated by the arrows, with each Fe being antiferromagnetically coupled to all its Fe nearest neighbors.

Zinc-blende FeAs [Fig. 1(b)] consists of interpenetrating face-centered-cubic sublattices of Fe and As that are shifted by $(\frac{1}{4},\frac{1}{4},\frac{1}{4})$ along the (111) direction relative to each other. As a result, both the Fe and As atoms are tetrahedrally coordinated, with corner-sharing polyhedra, and the packing density is lower than in the MnP case.

The calculated lattice parameters for MnP FeAs are given in Table I. Our calculations correctly obtain the AFM-ordered MnP structure as the ground state, with the zinc-blende-structure 1 eV per two-atom formula unit higher in energy. Figure 2(a) shows the relative stabilities of MnP-type and zinc-blende FeAs as a function of volume of a two-atom formula unit, set by uniformly scaling the equilibrium lattice parameters. The MnP-type structure is the ground state until

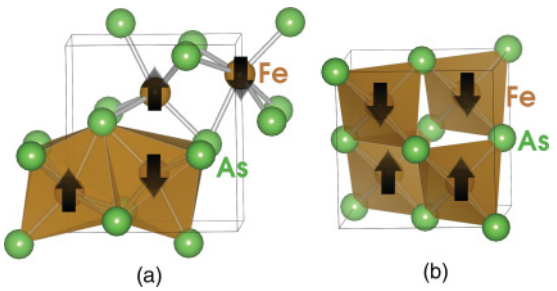

FIG. 1. (Color online) (a) Structure of MnP-type FeAs with ground-state AFM ordering indicated. (b) Structure of zinc-blende FeAs with arrows indicating ground-state AFM ordering.

TABLE I. Calculated and experimental crystal structure parameters for MnP-type FeAs and Cu_2Sb-type Fe_2As.

Parameter (Å)	FeAs GGA + U	FeAs Expt.[a]	Fe_2As GGA + U	Fe_2As Expt.[b]
a	5.471	5.442	3.627	3.627
b	3.276	3.372	3.627	3.627
c	6.050	6.028	5.980	5.981
Fe(x)	0.0020	0.0027		
Fe(z)	0.202	0.1194	0.329	0.318
As(x)	0.201	0.1193		
As(z)	0.573	0.5774	0.266	0.266

[a]Experimental results from Ref. 30.
[b]Experimental results from Ref. 32.

an expanded volume of 40 Å^3 per two-atom formula unit. At the equilibrium lattice volume of GaAs (45 Å^3), the zinc-blende structure is the lowest-energy structure, suggesting that it could be the stable phase in coherently grown GaAs/FeAs heterostructures, although our calculated lattice constant for zinc-blende FeAs (5.36Å) is smaller than that of GaAs.

Also in Fig. 2(a) are the relative energies for various magnetic orderings of the zinc-blende FeAs structure. We compare the relative energies of non-spin-polarized, ferromagnetic, and antiferromagnetically ordered structures. A G-type AFM solution was obtained in all cases when the moments on the Fe sites were initialized to C-, A-, or G-type ordering and nonconstrained calculations were performed. Projection of the plane-wave states into the PAW sphere gave a local magnetic moment of 2.4μ_B per iron atom at the equilibrium lattice constant. This value is intermediate between high-spin

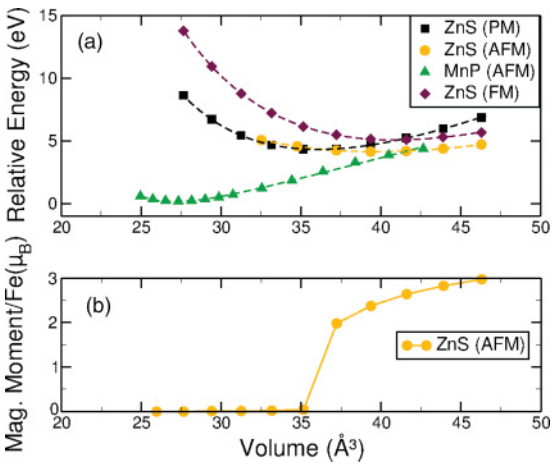

FIG. 2. (Color online) (a) Calculated energy-volume curves for MnP-type and zinc-blende FeAs with various types of magnetic orderings. The volume shown is for one two-atom formula unit of FeAs. The ferromagnetic (FM) curve was calculated by constraining the total moment to 11μ_B for four Fe ions. Antiferromagnetic ordering becomes stable above $V = 35$ Å^3 and remains more stable than FM with cell expansion. The MnP structure is stable over a large range of volumes. (b) Absolute value of magnetic moment per Fe for the zinc-blende structure with AFM ordering as a function of volume. Paramagnetic ordering is denoted by PM.

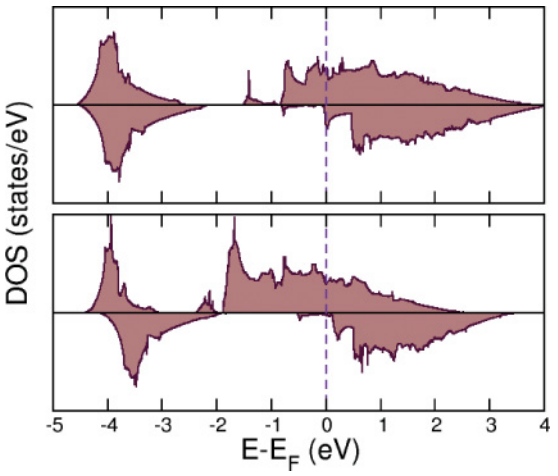

FIG. 3. (Color online) Spin-polarized density of states for hypothetical ferromagnetically ordered zinc-blende FeAs calculated at (a) the equilibrium volume of 38.5 Å^3 per two-atom formula unit and (b) at the experimental GaAs volume of 45 Å^3. The Fermi level is set to 0 eV.

and low-spin configurations for a nominally Fe^{3+} ion in a tetrahedral crystal field. Our FM solutions were obtained by fixing a total magnetic moment of $2.75\mu_B$ per Fe atom so as to avoid confusing multiple local minima; this value is obtained when a FM arrangement with initial magnetic moments of $3\mu_B$ per Fe is allowed to relax to its local minimum and is close to that obtained in our local projections for the AFM solutions. The paramagnetic results are obtained from a non-spin-polarized GGA calculation. We find that the antiferromagnetic or nonmagnetic solutions are lower in energy than the ferromagnetic over the entire volume range studied. The crossover between the AFM and nonmagnetic solutions corresponds to the volume collapse shown in Fig. 2(b).

Finally, to explore the spintronic properites, we calculated the spin-polarized density of states (DOS) for hypothetical ferromagnetically ordered zinc-blende FeAs at our calculated

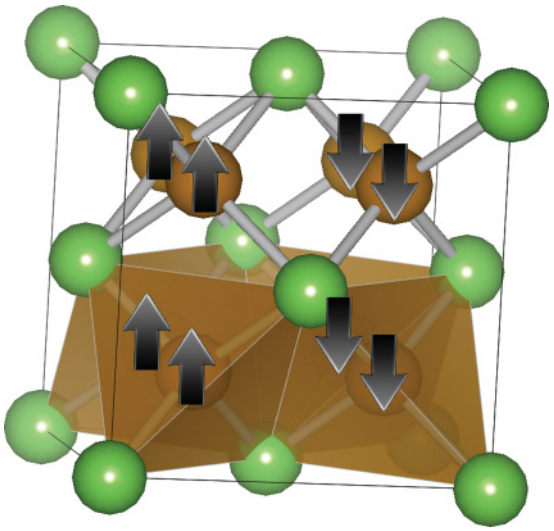

FIG. 4. (Color online) Fe_2As in the antifluorite structure. The calculated ground-state magnetic ordering is shown with arrows.

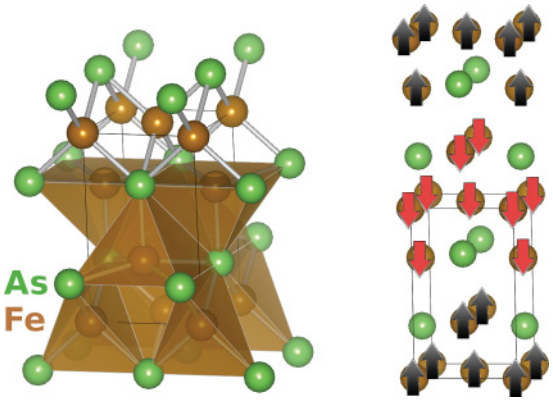

FIG. 5. (Color online) (a) Structure of Fe_2As in the Cu_2Sb structure. (b) Ground-state magnetic ordering of Cu_2Sb-type Fe_2As.

equilibrium volume (38.5 Å^3) and at the experimental volume of GaAs (45 Å^3) (Fig. 3). As expected, we find a narrowing of the bands as the volume is increased. In addition, the exchange splitting between majority and minority bands is more pronounced at the expanded volume, resulting in almost half-metallic behavior, similar to that previously reported for zinc-blende MnAs.[31] It is likely that half metallicity will be achieved with the additional band narrowing provided by quantum confinement in thin layers of FeAs in heterostructures.

B. Properties of bulk Fe_2As in antifluorite and Cu_2Sb structural variants

The Fe-pnictide superconductors consist of a layer of Fe_2As in the antifluorite structure sandwiched between a plethora of other constituents. Antifluorite (as opposed to fluorite because

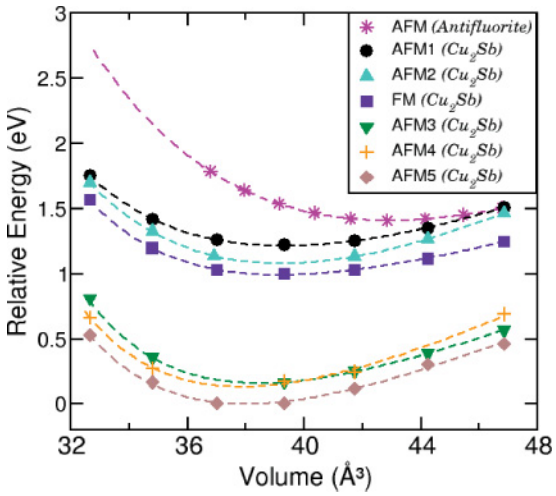

FIG. 6. (Color online) Calculated energy versus volume (of one three-atom formula unit) for the Cu_2Sb-type and antifluorite Fe_2As, for various magnetic orderings. Both were found to have AFM ground states, as shown in Figs. 4 and 5. The volume was varied by uniform scaling of the calculated equilibrium lattice parameters. The Cu_2Sb-type structure is stable across the whole range of volumes studied.

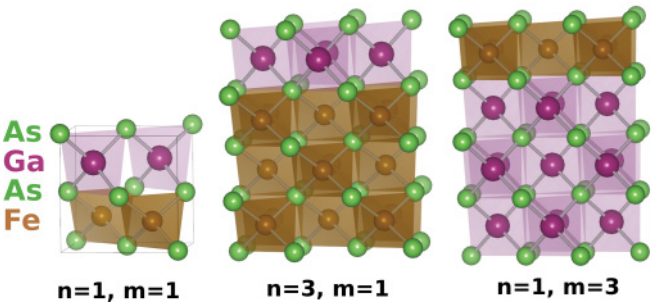

FIG. 7. (Color online) Zinc-blende-structure $(FeAs)_n$:$(GaAs)_m$ heterostructures studied in this work.

the anion and cation positions are exchanged) is made up of three interpenetrating face-centered-cubic sublattices with the Fe(I) sublattice shifted by $(\frac{1}{4},\frac{1}{4},\frac{1}{4})$ and the Fe(II) sublattice shifted by $(\frac{1}{4},\frac{3}{4},\frac{1}{4})$ along the (111) direction with respect to the As lattice at the origin. It can also be considered as stuffed zinc blende with four interstitial zinc-blende sites occupied with extra Fe atoms. The Fe and As atoms are tetrahedrally coordinated forming edge-shared tetrahedra as shown in Fig. 4.

In its ground state, bulk Fe_2As adopts the Cu_2Sb-type (C38) structure shown in Fig. 5(a).[32] There are two Fe cation sites Fe(I) and Fe(II), with each *a*-*b* plane containing a single cation type. These Fe(I) and Fe(II) planes are then alternated in the *c* direction. Half of the Fe ions are tetrahedrally coordinated with As and the others form octahedra with six neighboring As ions. These tetrahedra and octahedra are stacked to form an edge-sharing array.

Figure 6 shows the results of our energy-volume calculations for antifluorite and Cu_2Sb-type Fe_2As. The Cu_2Sb-type structure was found to be stable over the whole range of volumes calculated, with antifluorite Fe_2As less stable by 0.98 eV per formula unit compared to the ground state Cu_2Sb-type structure at its lowest-energy volume. Both calculations were carried out with their respective ground state AFM order. Our calculated structural parameters for the Cu_2Sb-type Fe_2As are compared with the experimental values in Table I.

For Cu_2Sb-type Fe_2As, DFT correctly obtains the experimentally determined magnetic ordering shown in Fig. 1(b).[33]

TABLE II. Calculated relative energies of different magnetic orderings (antiferromagnetic, ferromagnetic, and paramagnetic) in bulk zinc-blende FeAs and in zinc-blende FeAs/GaAs superlattices fixed to the experimental GaAs lattice parameter. All energies are per Fe atom and are relative to the ground-state AFM order. The values of the Fe magnetic moment *m* in the last column are those for the equilibrium AFM structure.

Structure	E_{AFM} (eV)	E_{FM} (eV)	E_{PM} (eV)	m (μ_B)
FeAs	0	0.174	0.209	2.15
$(FeAs)_1$:$(GaAs)_1$	0	0.181	0.482	2.89
$(FeAs)_1$:$(GaAs)_3$	0	0.010	0.345	2.82
$(FeAs)_1$:$(GaAs)_2$	0	0.246	0.323	2.68
$(FeAs)_3$:$(GaAs)_1$	0	0.115	0.202	2.52
$(FeAs)_2$:$(GaAs)_1$	0	0.207	0.280	2.63

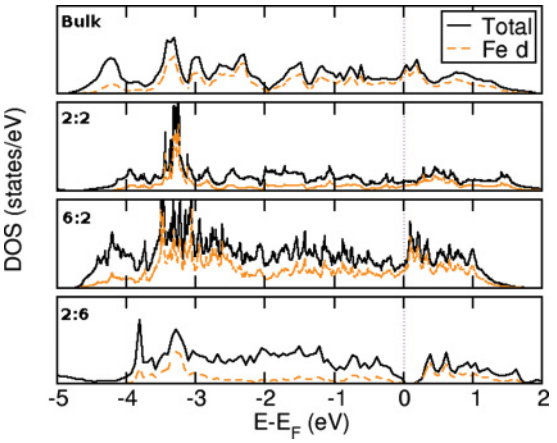

FIG. 8. (Color online) Calculated densities of states for zinc-blende-structure FeAs:GaAs heterostructures. The Fermi level is set to 0 eV in each plot and is indicated by the dotted line. The top panel shows bulk zinc-blende FeAs. Following from top to bottom are $(FeAs)_1(GaAs)_1$, $(FeAs)_3(GaAs)_1$, and $(FeAs)_1(GaAs)_3$. The total DOS is given by the solid black line. The orbital projected DOS for the Fe *d* states is given by the dashed orange line.

This is a trilayer A-type magnetic ordering consisting of three layers of ferromagnetically coupled Fe atoms coupled antiferromagnetically to the next three FM layers; the measured T_N is 353 K. The values of magnetic moment on the two inequivalent Fe sites were calculated to be $1.25\mu_B$ and $2.18\mu_B$, which are very close to the experimental values of $1.28\mu_B$ and $2.05\mu_B$.[34] This good agreement between the DFT GGA and experiment is significant because the magnitudes of the magnetic moments in pnictide superconductors are notoriously poorly reproduced by most flavors of density-functional theory. The next-lowest-energy magnetic ordering that we obtained in our calculations was another type of AFM ordering, with a destabilization energy of 0.4 eV per formula unit. For the range of volumes studied, no other magnetic ordering was found to be lower in energy than the experimentally found AFM ordering.

The calculated ground-state magnetic ordering for hypothetical bulk antifluorite Fe_2As was found to be type*A* with striped antiferromagnetically ordered single *a*-*b* plane layers coupled ferromagnetically in the *c* direction, as shown in Fig. 4. The next most stable ordering was FM, with a destabilization

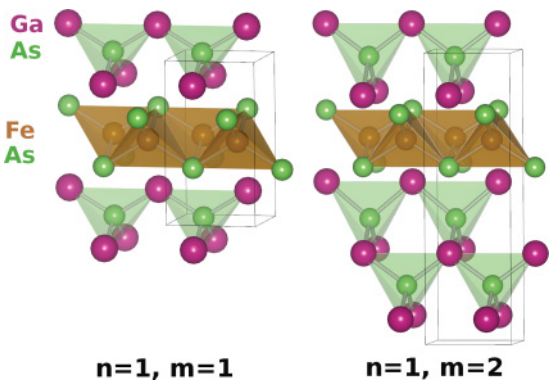

FIG. 9. (Color online) $(FeAs)_n$:$(GaAs)_m$ heterostructures for antifluorite FeAs on zinc-blende GaAs.

TABLE III. Calculated FeAs bond lengths and angles for antifluorite FeAs/zinc-blende GaAs superlattices.

Superlattice	Fe-As bond length (Å)	As-Fe-As bond angle (degrees)
Fe:Ga 1:1	2.36	106.6
		115.5
Fe:Ga 1:2	2.38	107.1
		114.3

energy in this case of only 0.17 eV per formula unit at the lowest-energy volume.

IV. RESULTS: FeAs/GaAs SUPERLATTICES

A. Zinc-blende FeAs/zinc-blende GaAs: Spintronic properties

While our calculations indicate that ferromagnetic order is not stable for bulk zinc-blende FeAs, we now consider whether it can be stabilized in thin films. We studied superlattices with alternating layers of zinc-blende-structure FeAs and GaAs (see Fig. 7). We relaxed the structures within the constraint of keeping the in-plane lattice parameter fixed at 5.65 Å, the experimental lattice parameter of GaAs. In all cases we obtained a checkerboard AFM ground state. Our calculated magnetic moments and relative total energies for different magnetic orderings for superlattices with different numbers of FeAs and GaAs layers are summarized in Table II.

For all of the calculated structures, the ground-state magnetic ordering is checkerboard antiferromagnetic. Increasing the ratio of FeAs layers to GaAs does not have an impact on the relative stability of the AFM order with repect to the FM order. The values of the magnetic moments are in the range of $2\mu_B$–$3\mu_B$ per Fe, which is very similar to that of bulk zinc-blende FeAs. The value of the magnetic moment increases as more layers of GaAs are added and seems to correlate with an increase in the out-of-plane Fe-As bond length as the number of GaAs layers is increased. To confirm this correlation we repeated the calculation with the Fe, Ga, and As ions in the ideal zinc-blende positions. Comparing the resulting magnetic moment magnitudes of the frozen bond lengths with those obtained by relaxing the ions shows that the increase in magnitude is not solely a result of quantum confinement, but is caused primarily by the larger Fe-As distance.

The densities of states for the FeAs:GaAs configurations of 1:1, 1:3, and 3:1 are compared with that of bulk zinc-blende FeAs in Fig. 8. Despite the change in heterostructure, the densities of states are very similar in the region surrounding the Fermi level. All except for the 3:1 superlattice are metallic with Fe states crossing the Fermi level. There is a broadband of Fe d states, with peaks at -3 and 0.5 eV. These Fe states hybridize with the As p states from the FeAs layers. There is only a small contribution from the As p states in the GaAs layers around the Fermi level. However, the main change in increasing the number of GaAs layers is to recover the semiconducting nature of the bulk GaAs material. A gap opens up in the $(FeAs)_1(GaAs)_3$ heterostructure, as shown in the bottom panel of Fig. 8.

In summary, all of the zinc-blende-structure FeAs/GaAs heterostructures that we have studied show robust antiferromagnetic ordering and are therefore unpromising for spintronic applications. Indeed, their absence of ferromagnetism and/or half metallicity might explain the experimental difficulties associated with spin injection across the Fe-GaAs interface.

B. Antifluorite Fe_2As/zinc-blende GaAs: Possible superconducting behavior

The FeAs-based superconducting materials all have a signature nested Fermi surface comprising holes and pockets at the Fermi level, resulting from their isolated antifluorite Fe_2As layers. Here we investigate whether such a Fermi surface can be reproduced in antifluorite Fe_2As/zinc-blende GaAs heterostructures. We studied two specific superlattices, both with one layer of FeAs alternating with a single layer or two layers of GaAs (Fig. 9). Note that, while the bulk antifluorite structure has the formula Fe_2As, a 1:1 Fe:As ratio is obtained by taking a slice of the unit cell to reproduce the structure found in the superconducting compounds.

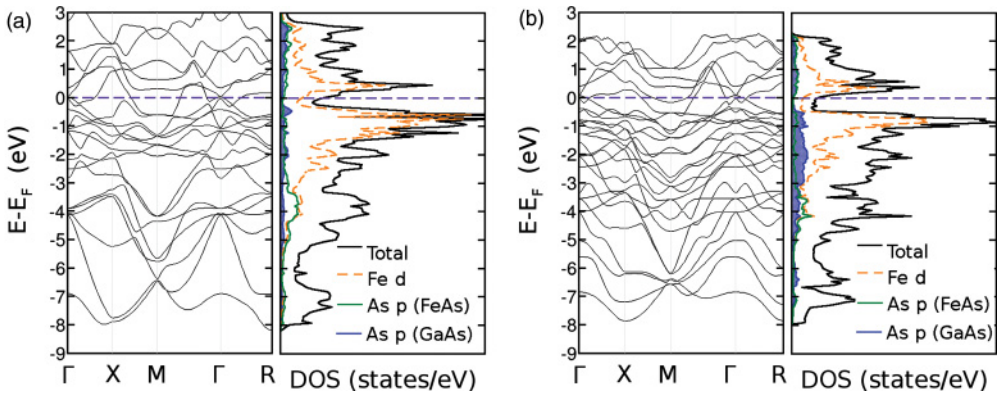

FIG. 10. (Color online) Band structures and densities of states for paramagnetic antifluorite Fe_2As/ zinc-blende GaAs superlattices. In all plots, the Fermi level is set to 0 eV. The total densities of states are given by the black line. The orbitally projected states of Fe d, As p (from the FeAs layers), and As p (from the GaAs layers) are shown by the dashed orange, green, and shaded blue lines, respectively. (a) Single-layer FeAs with single-layer GaAs. (b) Single-layer FeAs with double-layer GaAs.

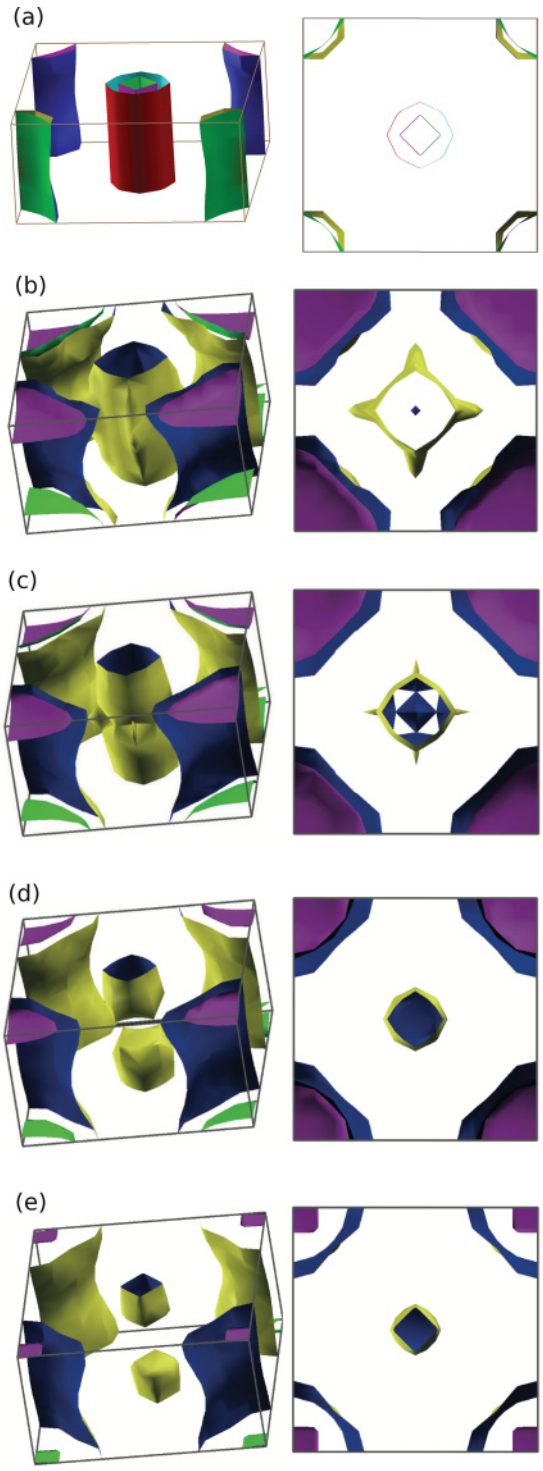

FIG. 11. (Color online) Fermi surface of LaOFeAs and FeAs/GaAs heterostructures for various levels of electron doping relative to the Fermi level: (a) LaOFeAs, (b) E_F, (c) $E_F - 0.1$ eV, (d) $E_F - 0.2$ eV, and (e) $E_F - 0.3$ eV.

First we calculate the equilibrium structures of the two heterostructures. As before, the in-plane lattice parameter was held fixed at the experimental GaAs lattice parameter of 5.65 Å and the out-of-plane lattice parameter and internal coordinates were relaxed with this constraint. In Table III we summarize our calculated Fe-As bond lengths and As-Fe-As bond angles; the latter have been previously shown to correlate with the superconducting transition temperature in the parent pnictide compounds, with angles closest to the ideal tetrahedral angle of 109.47° yielding the highest T_c.[35] Of the two heterostructures studied, we find that our $(FeAs)_1(GaAs)_2$ structure has an As-Fe-As bond angle closest to the ideal tetrahedral angle as a result of the slightly larger FeAs distance in the bilayer structure.

Next we evaluate the magnetic properties of the superlattices. We find that the antifluorite FeAs layer maintains several of its bulk magnetic characteristics as well as those of the Fe-pnictide superconductors. The ground-state magnetic ordering for both of the heterostructures was found to be striped antiferromagnetic, which is the same as both bulk Fe_2As and the Fe-pnictide superconducting parent compounds. The average calculated value of the magnetic moment on the Fe sites is $1.6\mu_B$, whereas for the Fe-pnictide compounds the calculated value varies between $1\mu_B$ and $2\mu_B$. However, experimentally the Fe magnetic moment value is less than half of these values. This known discrepancy between DFT and experiment is proposed to be a result of spin fluctuations and/or the ambiguity of precisely defining the magnetic form factor in a metal with itinerant magnetism. In view of this, we also expect our calculated values of the magnetic moment to be larger than those determined experimentally.

Finally, we calculated the electronic structures and Fermi surfaces of the two heterostructures. The band structures and densities of states of the two heterostructures in their paramagnetic state are shown in Fig. 10. In both cases we find electron and hole pockets in the Γ and M directions, which are characteristic features of the Fe-pnictide superconducting parent compounds.

As in the pnictide superconductors, the regions surrounding the Fermi level comprise Fe d and As p states. In contrast, however, we find contributions close to the Fermi level from components other than the Fe-As layers, in particular from As p states derived from the GaAs layers at −0.5 eV. This contribution increases with the addition of more layers of GaAs.

In Fig. 11 we show our calculated Fermi surface,and its variation with doping using a rigid band model, for the heterostructure with double layers of GaAs. In order to compare it to the protypical Fe-pnictide superconducting parent compound, we also include the Fermi surface for LaOFeAs at zero doping. The Fermi surface of the FeAs/GaAs heterostructure shares some features with the superconducting Fe-pnictide surfaces: At E_F, the center of the Brillouin zone consists of a distorted cylinder with a sphere nested inside. The zone edges have another cylinder with pockets at the corners. Reducing the electron count, the inner sphere disappears and the cylinders begin to shrink. At an energy of 0.2 eV below the Fermi level, the central cylinder splits into two cylindrical shapes. Unlike the superconducting pnictides, however, single cylinders rather than double cylinders occur at the Γ and M points. Therefore, the characteristic Fe-pnictide nesting between the zone center and zone edges cannot occur. In addition, the surface is manifestly three dimensional, whereas that of the superconductors is two dimensional.

V. CONCLUSION

We studied two types of FeAs/GaAs heterostructures, both with GaAs in the zinc-blende structure and with FeAs in the antifluorite structure or the zinc-blende structure. The zinc-blende/zinc-blende heterostructures allowed us to investigate possible spintronic applications of FeAs/GaAs. Our calculations suggest that desirable half metallicity and/or ferromagnetism are unlikely, however. Instead, the robustly stable AFM ordering offers a possible explanation for the failure of spin injection across the Fe/GaAs interface. While this is detrimental to spin injection, it offers an alternative route to exchange-bias devices if incorporated into a more complicated heterostructure.

Antifluorite Fe_2As/GaAs heterostructures would allow direct integration of superconductors into III-V semiconductor technologies if they reproduced the key features of the Fe-pnictide superconductors. While we see several features in common with the ferropnictide superconductors—the same AFM ordering, Fe *d* and As *p* states around the Fermi energy, and some similarities in the positions of the hole pockets in Fermi surface—we find that covalent bonding with the As *p* states from the GaAs layers causes the Fermi surface to be unfavorably three dimensional and inhibits the electron-hole pocket nesting that is characteristic of the Fe-pnictide superconductors. A possible route to avoid this Fermi level mixing is to use a more dissimilar spacer layer than GaAs such as GaN.

ACKNOWLEDGMENTS

We thank Kris Delaney and James Rondinelli for helpful discussions. This work was supported by the Materials Research Science and Engineering Center Program of the National Science Foundation under Grant No. DMR05-20415 and ETH Zurich. We also made use of the California NanoSystems Institute Computing Facility (Hewlett Packard) and Teragrid.

*sgriffin@ethz.ch; http://sites.google.com/sineadv0
†nicola.spaldin@mat.ethz.ch; http://www.theory.mat.ethz.ch

[1] G. A. Prinz, Science **250**, 1092 (1990).
[2] H. Munekata, H. Ohno, S. von Molnar, A. Segmuller, L. L. Chang, and L. Esaki, Phys. Rev. Lett. **63**, 1849 (1989).
[3] H. Ohno, A. Shen, F. Matsukura, A. Oiwa, A. Endo, S. Katsumoto, and Y. Iye, Appl. Phys. Lett. **69**, 363 (1996).
[4] M. Shirai, Physica E **10**, 143 (2001).
[5] G. Rahman, S. Cho, and S. C. Hong, J. Magn. Magn. Mater. **304**, 146 (2006).
[6] Y. Kamihara, T. Watanabe, M. Hirano, and H. Hosono, J. Am. Chem. Soc. **130**, 3296 (2008).
[7] G. A. Prinz, Science **282**, 1660 (1998).
[8] H. Ohno, Science **281**, 951 (1998).
[9] G. A. Prinz, G. T. Rado, and J. J. Krebs, J. Appl. Phys. **53**, 2087 (1982).
[10] M. W. Ruckman, J. J. Joyce, and J. H. Weaver, Phys. Rev. B **33**, 7029 (1986).
[11] M. Rahmoune, J. P. Eymery, and M. F. Denanot, J. Magn. Magn. Mater. **175**, 219 (1997).
[12] B. Lepine, S. Ababou, A. Guivarch, G. Jezequel, S. Deputier, R. Guerin, A. Filipe, A. Schuhl, F. Abel, C. Cohen, A. Rocher, and J. Crestou, J. Appl. Phys. **83**, 3077 (1998).
[13] B. D. Schultz, H. H. Farrell, M. M. R. Evans, K. Lüdge, and C. J. Palmstrøm, J. Vac. Sci. Technol. B **20**, 1600 (2002).
[14] S. Mirbt, B. Sanyal, C. Isheden, and B. Johansson, Phys. Rev. B **67**, 155421 (2003).
[15] C. Wang, L. Li, S. Chi, Z. Zhu, Z. Ren, Y. Li, Y. Wang, X. Lin, Y. Luo, S. Jiang, X. Xu, G. Cao, and Z. Xu, Europhys. Lett. **83**, 67006 (2008).
[16] M. R. Norman, Physics **1**, 21 (2008).
[17] B. T. Matthias, Phys. Rev. **92**, 874 (1953).
[18] B. T. Matthias, Phys. Rev. **97**, 74 (1955).
[19] G. Kresse and J. Furthmüller, Phys. Rev. B **54**, 11169 (1996).
[20] G. Kresse and D. Joubert, Phys. Rev. B **59**, 1758 (1999).
[21] P. E. Blochl, Phys. Rev. B **50**, 17953 (1994).
[22] J. P. Perdew, K. Burke, and M. Ernzerhof, Phys. Rev. Lett. **77**, 3865 (1996).
[23] J. P. Perdew, K. Burke, and M. Ernzerhof, Phys. Rev. Lett. **78**, 1396 (1997).
[24] H. J. Monkhorst and J. D. Pack, Phys. Rev. B **13**, 5188 (1976).
[25] S. L. Dudarev, G. A. Botton, S. Y. Savrasov, C. J. Humphreys, and A. P. Sutton, Phys. Rev. B **57**, 1505 (1998).
[26] S. M. Griffin and N. A. Spaldin (unpublished).
[27] I. I. Mazin, M. D. Johannes, L. Boeri, K. Koepernik, and D. J. Singh, Phys. Rev. B **78**, 085104 (2008).
[28] Z. P. Yin, S. Lebègue, M. J. Han, B. P. Neal, S. Y. Savrasov, and W. E. Pickett, Phys. Rev. Lett. **101**, 047001 (2008).
[29] A. C. Walters, T. G. Perring, J.-S. Caux, A. T. Savici, G. D. Gu, C.-C. Lee, W. Ku, and I. A. Zaliznyak, Nature Phys. **5**, 867 (2009).
[30] K. Selte and A. Kjekshus, Acta Chem. Scand. **23**, 2047 (1969).
[31] S. Sanvito and N. A. Hill, Phys. Rev. B **62**, 15553 (2000).
[32] K. Adachi and S. Ogawa, in *Magnetic Properties of Pnictides and Chaicogenides*, edited by H. P. J. Wijn, Landolt-Börnstein, New Series Group III, Vol. 27, Pt. a (Springer, Berlin, 1988).
[33] H. Katsuraki, J. Phys. Soc. Jpn. **19**, 1988 (1964).
[34] T. Matsushita, A. Kimura, H. Daimon, S. Suga, T. Kanomata, and T. Kaneko, Jpn. J. Appl. Phys. **31**, 1767 (1992).
[35] C.-H. Lee, A. Iyo, H. Eisaki, H. Kito, M. T. Fernandez-Diaz, T. Ito, K. Kihou, H. Matsuhata, M. Braden, and K. Yamada, J. Phys. Soc. Jpn. **77**, 083704 (2008).